Available online at www.sciencedirect.com
ScienceDirect
Trans. Nonferrous Met. Soc. China 30(2020) 2107−2118
Transactions of Nonferrous Metals Society of China
www.tnmsc.cn

Incipient melting phase and its dissolution kinetics for a new superalloy

Xin-xu LI[1,2], Chong-lin JIA[2], Yong ZHANG[2], Shao-min LÜ[2], Zhou-hua JIANG[1]

1. School of Metallurgy, Northeastern University, Shenyang 110819, China;
2. Aero Engine Corporation of China, Beijing Institute of Aeronautical Materials, Beijing 100095, China

Received 11 December 2019; accepted 3 June 2020

Abstract: Based on XRD, SEM and EDS analyses, the phases in GH4151 alloy were identified. Differential scanning calorimetry (DSC) experiment and metallographic method were carried out to determine the incipient melting temperature (IMT) of the alloy. The result shows that the IMT of alloy is situated between 1150 and 1160 °C. Subsequently, the dissolution process of Laves phase was carried out, and the dissolution kinetic equations were obtained at different temperatures. And then based on the verification of experiments, the model was confirmed to be credible to predict the fraction of the Laves phase dissolution. Finally, the results of diffusion coefficients indicate that the diffusion of Nb element is a critical factor for homogenization process of GH4151 alloy.
Key words: GH4151 ingot; homogenization; incipient melting; Laves phase; kinetics

1 Introduction

Nickel-based superalloys are important materials used to manufacture the critical components which operate in severe environments for the high-temperature and load-bearing service applications [1−3]. The increased thrust-to-weight ratio in the advanced aircraft demands higher inlet temperature and increased efficiency for the turbine [4], which requires excellent thermal and mechanical properties of the superalloy. In order to meet the critical demands for high temperature applications, some refractory and strengthened elements such as Nb and Mo are added into superalloy [5]. However, due to their different atomic sizes and segregation inclination, severe micro-segregation and undesirable topologically close-packed (TCP) phases will form in many as-cast Ni-based superalloys [6,7]. TCP precipitates are rich in refractory elements such as W, Co, Cr and Mo, so precipitates in the austenite matrix and the heavily solute concentration regions are highly detrimental to fatigue life of superalloy [8−10]. GH4151 alloy is a newly developed γ' precipitation strengthened nickel-based wrought superalloy, whose optimized compositions have been designed with 3.4 wt.% Nb and total content of Al, Ti, Nb up to around 10 wt.%. Such a high alloying degree would inevitably lead to greater segregation coefficient and promote the formation of harmful phase. Severe segregation inclination could adversely affect subsequent processing, so it is very necessary to eliminate harmful phases and alleviate segregation degree before subsequent processing.

Studies have shown that the homogenization heat treatment plays a key role in the elimination of the segregation and obtaining the homogenized microstructure so as to improve the formability of ingots for further processing or hot working [11−14]. The low temperature homogenization stage is routine procedure in an industrial practice that is conducted to avoid incipient melting. In general, incipient melting during homogenization heat

Foundation item: Project (50974016) supported by the National Natural Science Foundation of China
Corresponding author: Chong-lin JIA; Tel: +86-13021171768; E-mail: biamjcl@163.com
DOI: 10.1016/S1003-6326(20)65364-X

treatment is considered as detrimental to the mechanical properties [15−17]. However, lower temperature will certainly influence the diffusion process of elements. Therefore, the first stage for homogenization is proceeded to obtain the highest possible temperatures in order to ensure the highest possible diffusion coefficients without triggering incipient melting. However，it is quite difficult to identify the temperature of incipient melting for high alloying as-cast superalloys. What's more, complex precipitates make the determination of initial melting point more difficult due to high alloying elements of GH4151 alloy. In order to determine the incipient melting of the materials, differential scanning calorimetry (DSC) experiments were carried out as a typical method. LASA and RODRIGUEZ-IBABE [18] monitored the dissolution of the Al2Cu phase in two Al−Si−Cu−Mg casting alloys using calorimetry, with the aim of investigating the possibility of using DSC analysis to optimize solution heat treatment in high Cu-content Al−Si−Cu−Mg alloy. However, it has been reported that it is quite difficult to identify the solvus and solidus temperatures of as-solidified superalloys from DSC profiles due to broadening of the corresponding endothermic and exothermic peaks caused by chemical heterogeneity [16]. To overcome this problem, metallographic method was applied to determining the incipient melting temperature (IMT) for as-cast ingot. MIAO et al [19] reported that the IMT of *d*406 mm Inconel 718 ingot is situated between 1170 and 1180 °C by using metallographic method. In addition to the fact that the diffusion coefficient of elements varies greatly with temperature, the dissolution rate of Laves phase is also greatly affected by temperature. Therefore, it is very significant to conduct quantitative analysis for dissolution process of incipient melting phase. However, at present, few investigations have focused on IMT precisely and the kinetics analysis of Laves phase dissolution in such a highly alloyed and high γ' volume fraction GH4151alloy.

The present study is focused on GH4151 superalloy with excellent thermal and mechanical properties. The investigation of homogenization on GH4151 alloy is meaningful as the guidance for commercial application. The experiment was designed to take an initial step to determine the temperature of incipient melting and calculate the kinetics of Laves phase dissolution based on the Johnson−Mehl−Avrami−Kolmogorov (JMAK) analysis at different temperatures and soaking time.

2 Experimental

2.1 Processing

The as-cast *d*350 mm GH4151 ingot was prepared by vacuum induction melting and vacuum arc remelting with chemical composition as shown in Table 1. The sample of 8 mm × 20 mm × 40 mm was cut from ingot and electrolyzed on the DC power device. The electrolyte was $C_3H_8O_3$(50 mL) +HCl(50 mL)+$C_6H_8O_7$ (10 g)+CH_3OH(900 mL), the current density was 0.1−0.2 A/cm^2, and the electrolytic temperature was 0−5 °C. The anode sludge was washed 3 times with citric acid aqueous solution and distilled water, cleaned with methanol, and then pumped and dried with 0.2 μm organic filter membrane. The powder obtained was tested on D8 Discover XRD equipment, and the results were calibrated on Jade 6.5.

Table 1 Main chemical composition of GH4151 alloy (wt.%)

Al	Ti	Nb	Cr	Mo	W	V	C	Ni
3.8	2.8	3.5	11.2	4.4	2.6	0.6	0.07	Bal.

Small rectangular samples (10 mm×10 mm× 5 mm) were cut from the center of ingot for homogenization treatment. A muffle furnace having the temperature control system with the accuracy of ±3 °C was used for these thermal treatments. The samples were soaked at 1100, 1130, 1140, 1150, 1160, 1170, 1180 and 1190 °C for 1 h and then quenched in water. The parameter of homogenization was generated according to the incipient melting temperature determined by the metallographic method. To investigate the effect of homogenization parameters on the dissolution of Laves phase, the ingot was homogenized at 1050, 1100, 1140 and 1150 °C for different holding durations in order to calculate the dissolution kinetics of Laves phase. The samples were quenched in water for examining the microstructure evolution. Samples were ground and polished using standard sample preparation techniques for metallographic observations.

The differential scanning calorimetry (DSC)

experiment was carried out on a NETZSCH STA 404C instrument to reveal the incipient melting temperature of GH4151 alloy. The DSC sample was cut from as-cast ingot with dimensions of 4 mm × 1 mm and then placed in an alumina crucible and tested in an argon atmosphere. The maximum value of heating temperature was set as 1400 °C, while heating rate was controlled at 10 °C/min. Prior to the experiment, a heating curve was recorded as a baseline in the case of a crucible without the sample. The heating curves of the sample and crucible minus the baseline could be regarded as the heating curves of the sample. The incipient temperature was obtained on the heating curve.

2.2 Microstructure characterization

The microstructural features were revealed by Kalling's reagent (100 mL HCl + 100 mL ethanol + 5 g $CuCl_2$) as the standard chemical etchant for detection of dendritic structure and precipitates of nickel-based superalloy. Leica DM6000M optical microscope and Quanta 200FEG scanning electron microscope were employed to inspect micro-structure, and energy dispersive spectroscopy (EDS) was employed to perform semi-quantitative microanalysis of precipitates. The volume fraction of Laves phase in the quenched samples was measured by quantitative image analysis using the Photoshop software. An average of values obtained from five SEM micrographs was used to represent the fraction of Laves phase. The uncertainty of these measurements was estimated through independent calculation by different testers to be <5%.

3 Results and analysis

3.1 Analysis of as-cast ingot

The electrolytic extraction method was applied to characterizing the secondary precipitates. Most of γ phases and γ' phases were removed by electrolytic corrosion, and the obtained powders contained minor secondary phases of GH4151 alloy. As illustrated in Fig. 1, γ matrix, γ' phase, (Nb,Ti)C carbides, η phase, and Laves phase were identified in as-cast GH4151 alloy.

The optical micrographs taken from center sections of as-cast GH4151 ingot are shown in Fig. 2(a), and it can be seen that the microstructure presents an obvious dendrite structure, consisting of

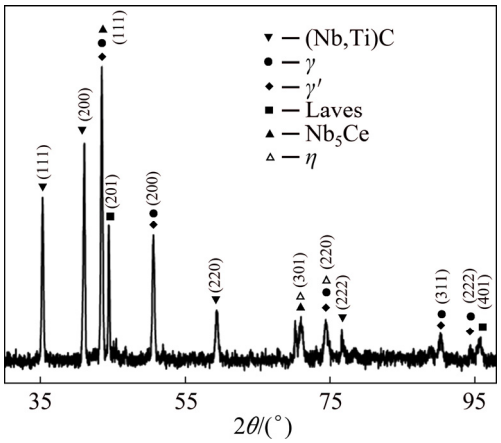

Fig. 1 XRD pattern of as-cast GH4151 alloy

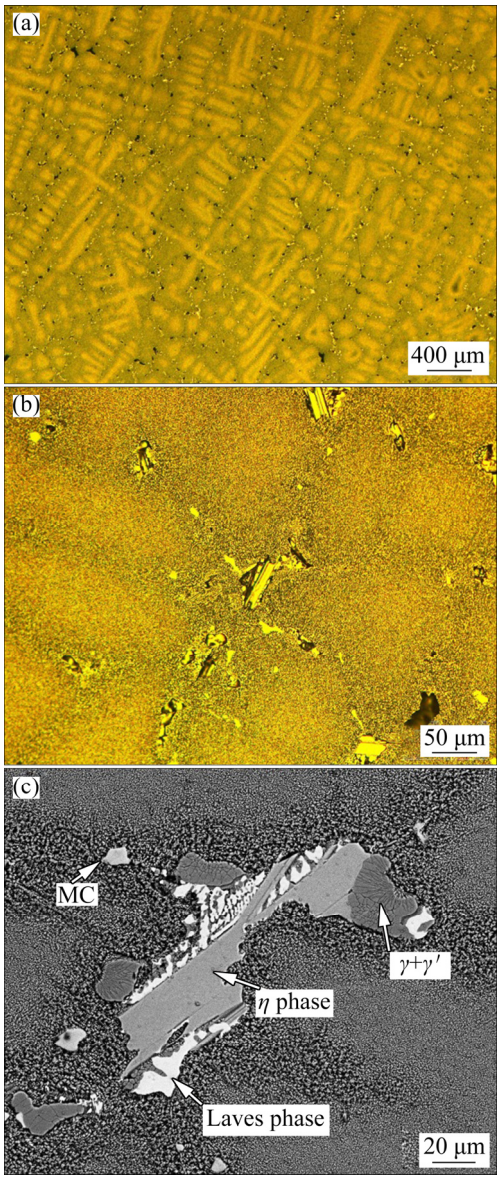

Fig. 2 Microstructures of GH4151 alloy: (a) Dendrite structure; (b) Secondary phases in OM; (c) Secondary phases in SEM

dendrite arms and interdendritic regions. The large secondary dendrite spacing implies that the segregation of GH4151 alloy is great. Moreover, the precipitates in interdendritic regions are complex as described in Fig. 2(b). In order to identify these secondary phases, scanning electron microscope (SEM) was employed to further obtain the morphologies, as illustrated in Fig. 2(c).

The EDS analyses of secondary phases are listed in Table 2. It was demonstrated that the secondary phases existing at interdendritic regions mainly consisted of Laves phase, (Nb,Ti)C phase (MC), η phase, and eutectic $\gamma+\gamma'$ phase. According to Table 2, the EDS results illustrate that Laves phases are rich in Co, Cr, Mo, and Nb, while MC carbides and η phases are both rich in Nb and Ti in as-cast GH4151 alloy. This also implies that high amounts of the major elements, including Nb, Cr, Co, Mo and Ti are concentrated in these precipitates. The concentrations of these elements in these phases are accompanied by their reduction in the matrix and inhomogeneity in the cast structure, consequently resulting in degraded mechanical properties.

As presented in Fig. 3, the EDS map scanning taken from Fig. 2(c) illustrates the distributions of

Table 2 EDS analysis of secondary phase (wt.%)

Phase	Ni	Co	Cr	W	Al	Mo	V	Nb	Ti	C
Laves	23.1	18.4	17.2	3.7	0.4	15.6	0.2	15.0	1.4	4.9
MC	4.3	2.3	0.1	2.8	–	2.6	–	58.8	13.3	15.7
$\gamma+\gamma'$	53.8	14.2	11.0	2.0	2.6	4.9	0.8	4.0	4.6	2.2
η	59.6	13.0	3.5	1.0	2.0	1.6	0.4	8.0	7.3	3.7

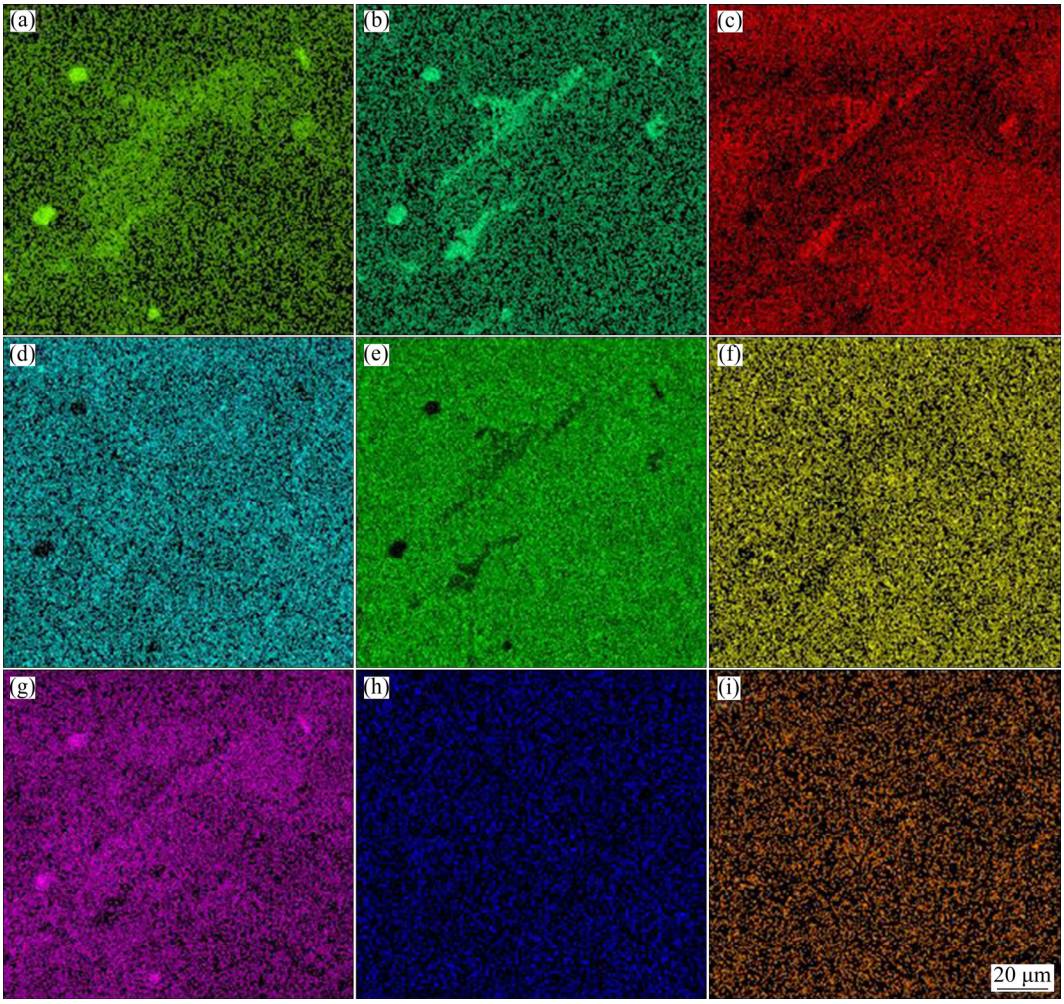

Fig. 3 Element map-scanning of selected region in Fig. 2(c): (a) Nb; (b) Mo; (c) Cr; (d) Co; (e) Ni; (f) Al; (g) Ti; (h) W; (i) V

the main alloying elements, including Nb, Mo, Cr, Co, Ni, Al, Ti, W, and V. In the as-cast GH4151 alloy, Nb, Ti, and Mo are significantly enriched in interdendritic region, while Al, Co, and Cr are enriched at dendritic arm. It can be seen that the Laves phase is enriched in Nb, Mo, Co and Cr, but its Ni, Al, and Ti contents are lower than those of the matrix. This indicates that the dissolution process of Laves phase is controlled by these elements, including Nb, Mo, Co and Cr. The η phase mainly consists of Ni, Ti, Nb and Co. According to their composition, these MC carbides particles can be written by (Nb,Ti)C.

3.2 Incipient melting temperature determination

Severe segregation inclination and formation of brittle precipitates could adversely degrade mechanical properties of the materials, so it is very necessary to eliminate harmful phases and segregation degree before subsequent processing. The low temperature homogenization stage is conducted to avoid incipient melting. Preliminary analysis of the incipient melting temperatures in the GH4151 alloy was carried out using DSC, as shown in Fig. 4(a), where exothermic peaks are represented in the upward direction. Figure 4(b) shows partial enlarged detail in Fig. 4(a). It can be seen that the incipient melting of GH4151 alloy is situated between 1158 and 1174 °C.

In addition, metallographic method was applied to further determining the IMT for *d*350 mm ingot. Figure 5 shows the microstructure evolution through different heating processes. According to the kinetic theory of phase transformation [20], non-equilibrium diffusion and the reduction of the phase interface are deem to be the original driving force leading to incipient melting. From Figs. 5(a−e), the fraction of Laves phase exhibits a decreasing tendency with increasing soaking temperatures while no obvious change is found concerning to the appearance of Laves phase. As illustrated in Fig. 5(f), incipient melting appeared around some areas of large Laves phase when the soaking temperature was raised to 1160 °C. Only bigger particles were dissolved when the temperature reached dissolving temperature due to the non-equilibrium diffusion and insufficient solution time. When the temperatures reach 1170, 1180 and 1190 °C, γ/Laves eutectic was observed,

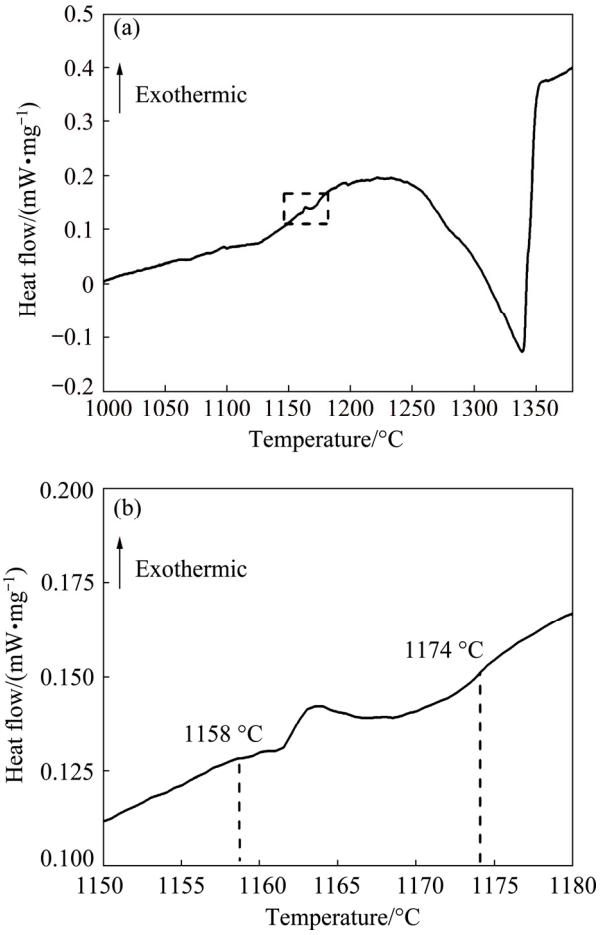

Fig. 4 Results from differential scanning calorimetry of GH4151 alloy (Heating rate: 10 °C/min)

as shown in Figs. 5(g−i). This phenomenon indicates that all of the Laves phases have melted when soaked at these temperatures. Detailed SEM morphologies of γ/Laves eutectic were the result of water quenching, as presented in Fig. 6. From the above analysis, it can be inferred that the IMT of *d*350 mm GH4151 ingot is situated between 1150 and 1160 °C and the result is in accordance with that of DSC, and then the subsequent homogenization temperature should be lower than 1160 °C.

3.3 Time and temperature dependent homogenization model for elimination of Laves phase

As stated above, it has been revealed that homogenization temperature should be lower than 1160 °C. According to the fundamental atomic diffusion theory [21], temperature and diffusing time play a significant role in dissolution process of

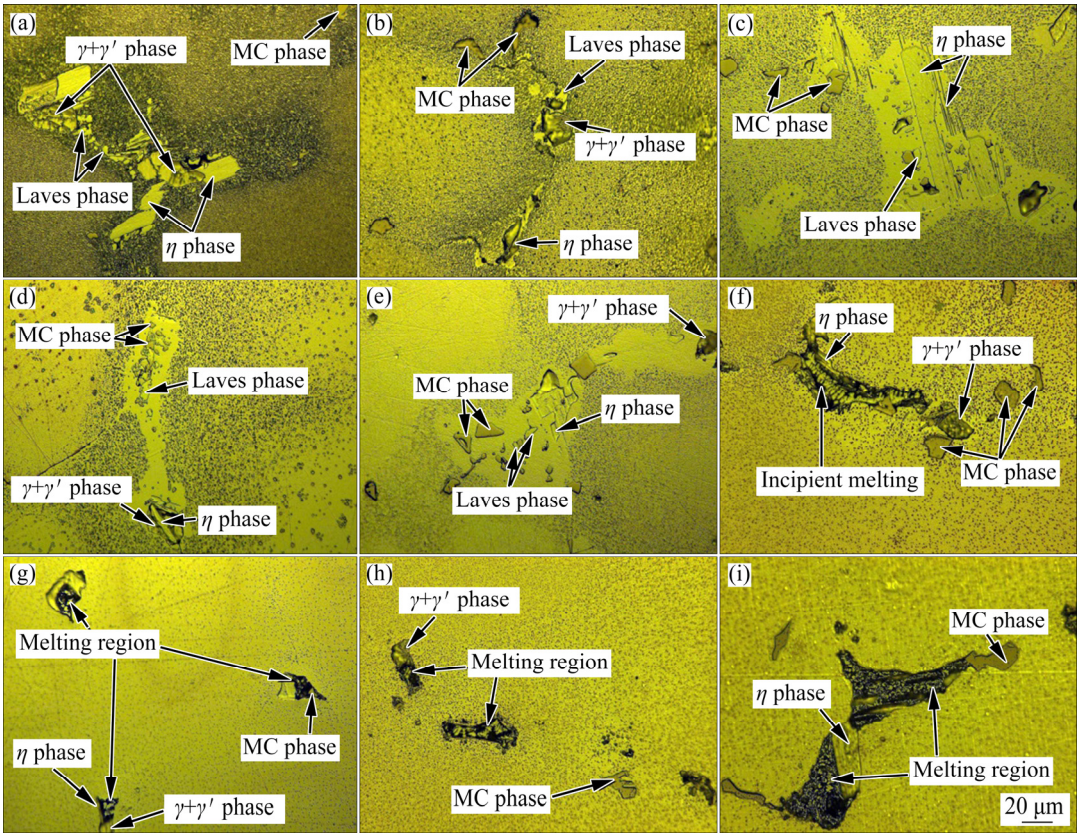

Fig. 5 Microstructures of as-cast alloy soaked at 1100 °C (a), 1120 °C (b), 1130 °C (c), 1140 °C (d), 1150 °C (e), 1160 °C (f), 1170 °C (g), 1180 °C (h) and 1190 °C (i) for 1 h and then quenched in water

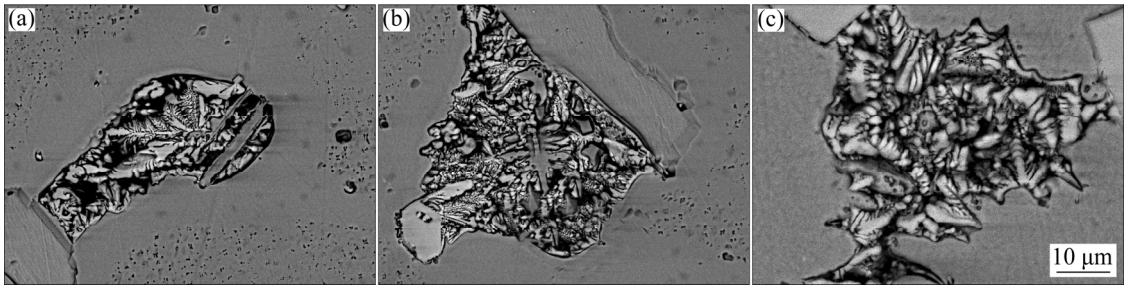

Fig. 6 Microstructures of γ/Laves eutectic soaked at 1170 °C (a), 1180 °C (b) and 1190 °C (c) for 1 h and then quenched in water

Laves phase. Figure 7 shows the morphology of Laves phase in as-cast ingot and the microstructure evolution at 1050 °C for different soaking time. With the proceeding of homogenization, Laves phase gradually disappeared. However, when the homogenization time reached 26 h at 1050 °C, a little Laves phase still existed. This indicates that the dissolving rate of Laves phase is very low due to low diffusion rate of elements at 1050 °C.

In order to enhance diffusion rate of elements, homogenization temperature needs to be further increased. Figure 8 shows the microstructure evolution of Laves phase at 1100 °C for different soaking time. With the proceeding of homogenization at 1100 °C, Laves phase gradually decreased. Compared with the results of homogenization at 1050 °C, it required less time to dissolve Laves phase at 1100 °C. However, homogenization temperature still needs to be raised to reduce soaking time.

In order to avoid IMT of alloy, the next homogenization temperature is set at 1140 °C. When the homogenization time reached 10 h at 1140 °C, no Laves phase was observed, as shown in Fig. 9.

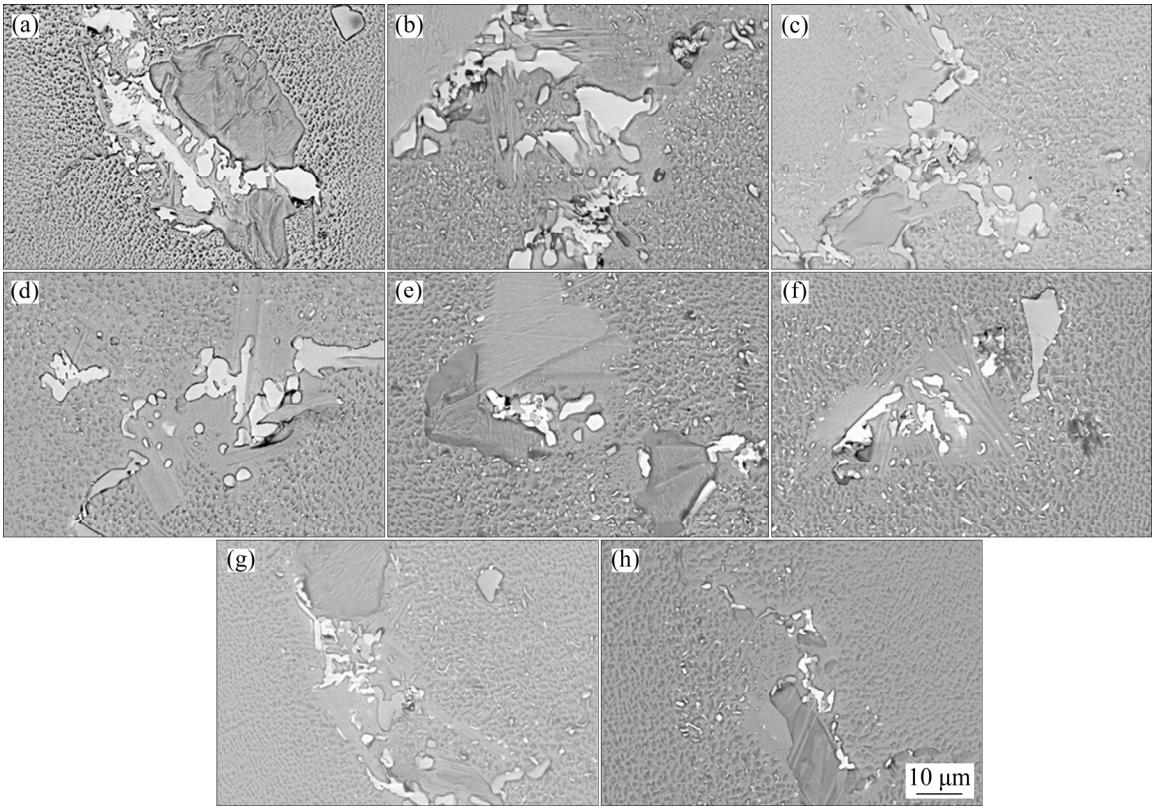

Fig. 7 Laves phase morphology in as-cast ingot and microstructure evolution treated at 1050 °C for different soaking time: (a) Ingot; (b) 2 h; (c) 6 h; (d) 10 h; (e) 15 h; (f) 20 h; (g) 23 h; (h) 26 h

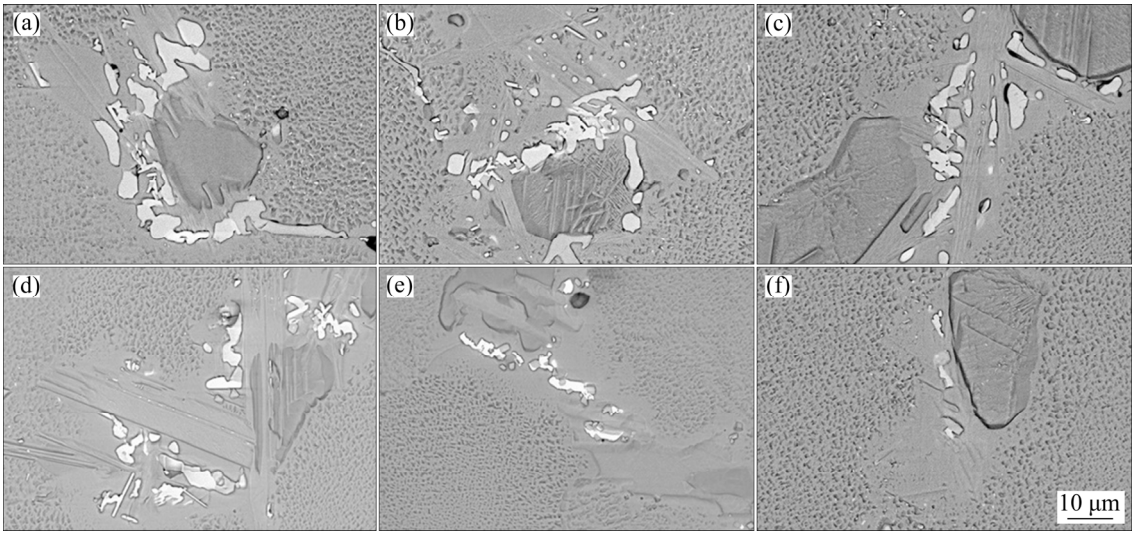

Fig. 8 Microstructure evolution of Laves phase treated at 1100 °C for different soaking time: (a) 1 h; (b) 3 h; (c) 7 h; (d) 9 h; (e) 12 h; (f) 16 h

There is no incipient melting inclination at all at 1140 °C, so the homogenization temperature could be increased to 1150 °C. Figure 10 shows the microstructure evolution at 1150 °C for different soaking time. It can be seen that when the homogenization time reached 8 h at temperature of 1150 °C, Laves phase disappeared. Because the IMT of *d*350 mm GH4151 ingot is situated between 1150 and 1160 °C, homogenization temperature cannot continue to increase.

When the homogenization time reached 10 and 8 h at temperature of 1140 and 1150 °C, respectively,

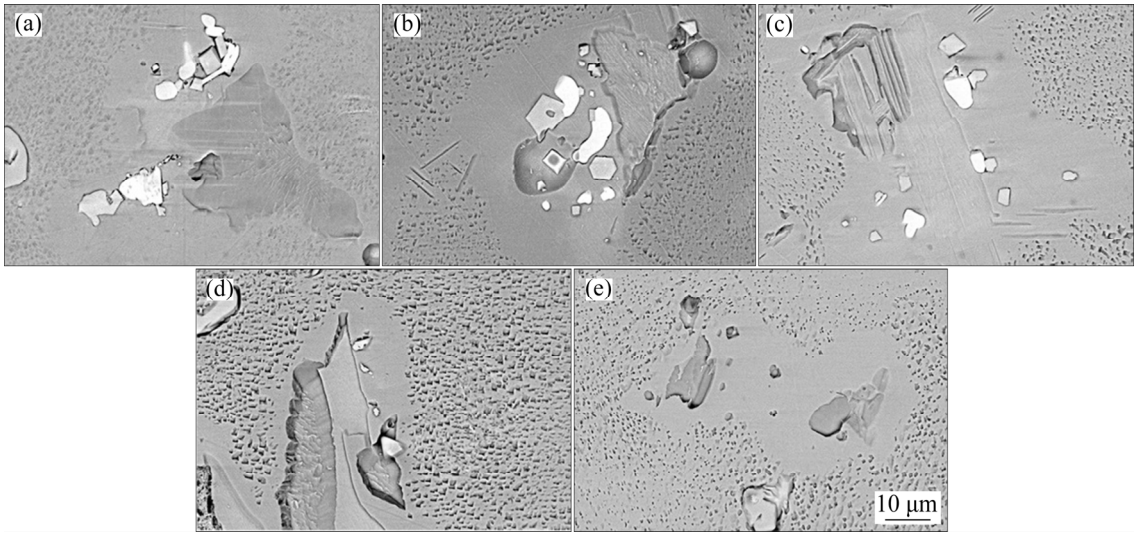

Fig. 9 Microstructure evolution of Laves phase treated at 1140 °C for different soaking time: (a) 1 h; (b) 3 h; (c) 5 h; (d) 7 h; (e) 10 h

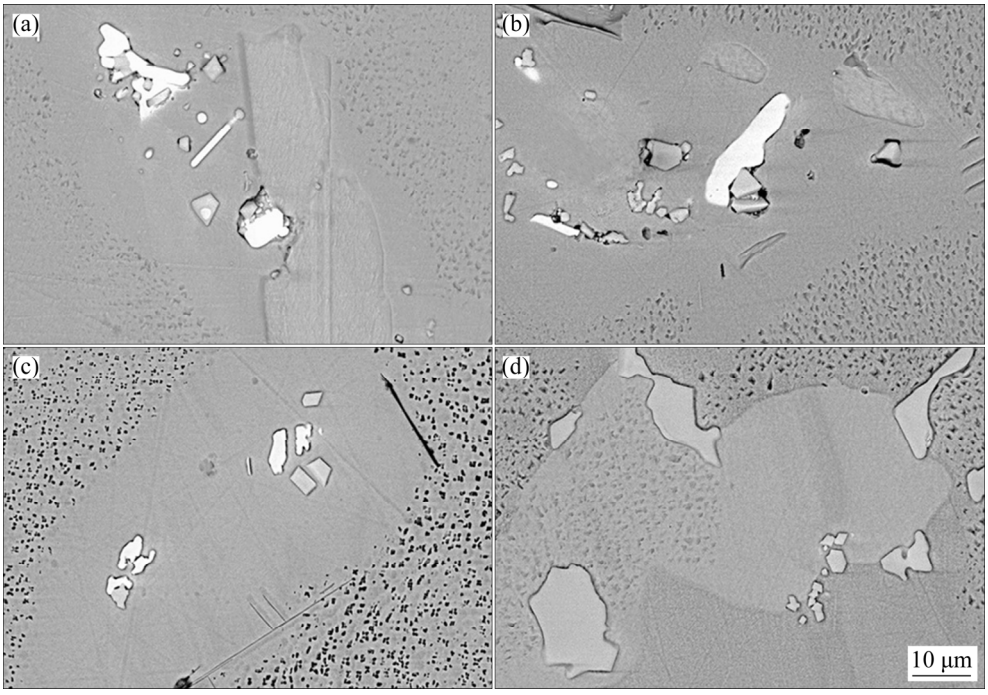

Fig. 10 Microstructure evolution of Laves phase treated at 1150 °C for different soaking time: (a) 1 h; (b) 3 h; (c) 5 h; (d) 8 h

no Laves phase was observed, as shown in Figs. 9 and 10. While the homogenization time reached 26 and 12 h at temperatures of 1050 and 1100 °C, respectively, a little Laves phase still existed. This indicates that homogenization treatment at high temperature plays an essential role in dissolving Laves phase.

In order to predict the Laves phase dissolution process at different temperatures and time, the kinetics of Laves phase dissolution can be modeled by the Johnson–Mehl–Avrami–Kolmogorov (JMAK) equation [22−24]:

$$X=1-\exp(-Kt^n) \quad (1)$$

where X is the dissolute fraction of Laves phase, n is the Avrami exponent, K is a temperature-dependent coefficient, and t is the time. The values of X were calculated based on Eq. (2):

$$X=(S_0-S)/S_0 \quad (2)$$

where S_0 and S are related to the initial fraction for

as-cast ingot and the current fraction of Laves phase in the certain area, respectively. By algebraic transformation, the following equation can be obtained:

$$\ln\left[\ln\left(\frac{1}{1-X}\right)\right]=\ln K+n\ln t \tag{3}$$

As a result, the value of $\ln K$ could be determined by the intercept of the plot of $\ln\{\ln[1/(1-X)]\}$ versus $\ln t$. The corresponding plot is illustrated in Fig. 11, where the values of $\ln K$ were obtained as −2.19105, −1.21084, −0.58255 and −0.35401 at the temperatures of 1050, 1100, 1140 and 1150 °C, respectively. Meanwhile, the values of n were also obtained as 0.73389, 0.66695, 0.56268, and 0.49318 at the temperatures of 1050, 1100, 1140 and 1150 °C, respectively.

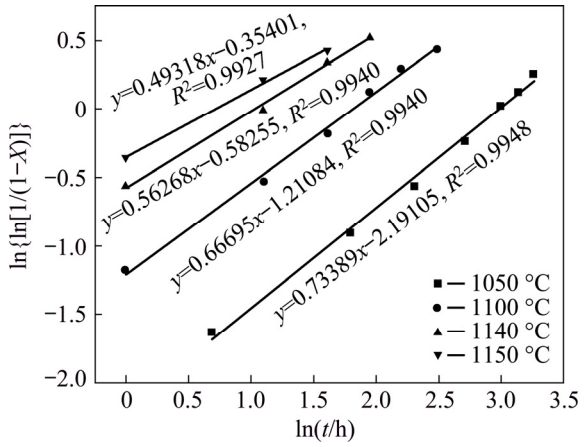

Fig. 11 Avrami plots for dissolution of Laves phase at different temperatures

Therefore, the kinetic equations of Laves phase dissolution can be deduced at the temperatures of 1050, 1100, 1140 and 1150 °C, respectively. And then the following equations can be obtained:

$$X=1-\exp(-0.1118t^{0.73389})\ (1050\ ^\circ\mathrm{C}) \tag{4}$$

$$X=1-\exp(-0.2979t^{0.66695})\ (1100\ ^\circ\mathrm{C}) \tag{5}$$

$$X=1-\exp(-0.5585t^{0.56268})\ (1140\ ^\circ\mathrm{C}) \tag{6}$$

$$X=1-\exp(-0.7019t^{0.49318})\ (1150\ ^\circ\mathrm{C}) \tag{7}$$

In order to predict the Laves phase elimination process at different temperatures, it is assumed that the Laves phase elimination process is completed when the dissolute fraction of Laves phase is 99%. According to Eqs. (6) and (7), it can be deduced that when the homogenization time reached 10 and 8 h at temperatures of 1140 and 1150 °C, respectively, Laves phase should be eliminated, as presented in Figs. 9 and 10. According to Eqs. (4) and (5), the homogenization time reached 32 and 20 h at temperatures of 1050 and 1100 °C, respectively, there should exist no Laves phase in the microstructure. The fact can be illustrated in Fig. 12. Therefore, the relationship obtained from JMAK equation is valid to predict the fraction of the dissolution of Laves phase for GH4151 alloy.

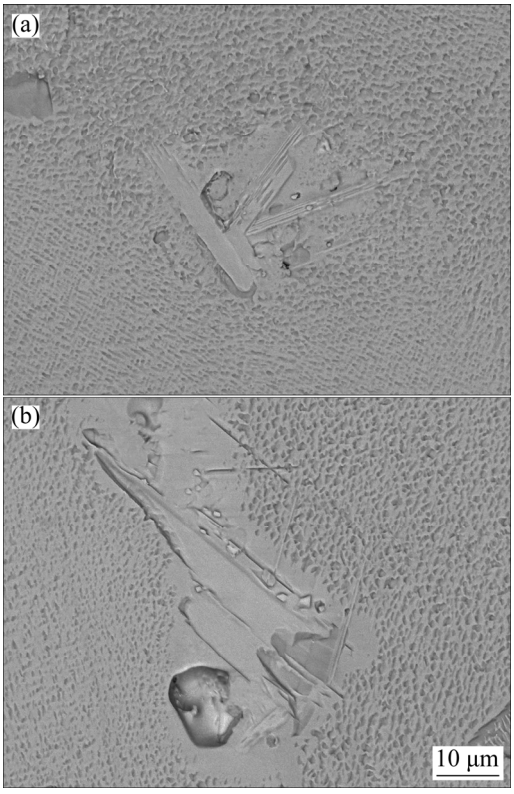

Fig. 12 Microstructure evolution of alloy during homogenization at 1050 °C for 32 h (a) and at 1100 °C for 20 h (b)

3.4 Element segregation in dendritic structure during homogenization

In addition to the elimination of Laves phase, elimination of micro-segregation is also an important issue for homogenization treatment. In order to identify the effect of homogenization, the concept of residual segregation index δ is introduced. The following equation [25] was used to express the relationship between dendrite spacing L and element diffusion coefficient D at homogenization temperature, homogenization time t and index δ:

$$\delta=\frac{c_{\max}^{t}-c_{\min}^{t}}{c_{\max}^{0}-c_{\min}^{0}}=\exp(-\frac{4\pi^2}{L^2}Dt) \tag{8}$$

where $c_{\max}^{t}$ and $c_{\min}^{t}$ are the maximum and minimum concentrations after homogenization, respectively, and $c_{\max}^{0}$ and $c_{\min}^{0}$ are the maximum and minimum concentrations before homogenization, respectively.

By algebraic transformation, the following equation can be obtained:

$$\ln\delta=-\frac{4\pi^2}{L^2}Dt \tag{9}$$

Table 3 shows the change of residual segregation index (δ) homogenized at 1150 °C for 8 h.

Then, diffusion coefficients (D) were calculated by fitting the linear relationship between ln δ and t, which is described in Fig. 13. The results show that diffusion coefficients of Nb, Ti, Mo, W were obtained as 2.86×10^{-11}, 5.09×10^{-11}, 3.16×10^{-11}, and 3.92×10^{-11} cm^2/s, respectively. Therefore, this indicates that severe segregation and low diffusion coefficient of Nb contributed to the difficulties in homogenization treatment of GH4151 alloy.

Table 3 Element content and residual segregation index (δ) during homogenization

Time/h	Nb			Ti			Mo			W		
	$c_{\max}^{t}$/%	$c_{\min}^{t}$/%	δ	$c_{\max}^{t}$/%	$c_{\min}^{t}$/%	δ	$c_{\max}^{t}$/%	$c_{\min}^{t}$/%	δ	$c_{\max}^{t}$/%	$c_{\min}^{t}$/%	δ
1	5.27	2.11	0.90	3.71	1.69	0.89	5.46	3.62	0.81	3.63	2.14	0.89
3	4.99	2.13	0.82	3.58	1.79	0.79	5.39	3.68	0.76	3.55	2.19	0.81
5	4.90	2.21	0.77	3.49	1.96	0.68	5.33	3.79	0.68	3.46	2.25	0.72
8	4.82	2.41	0.69	3.38	2.11	0.56	5.19	3.81	0.61	3.38	2.34	0.62

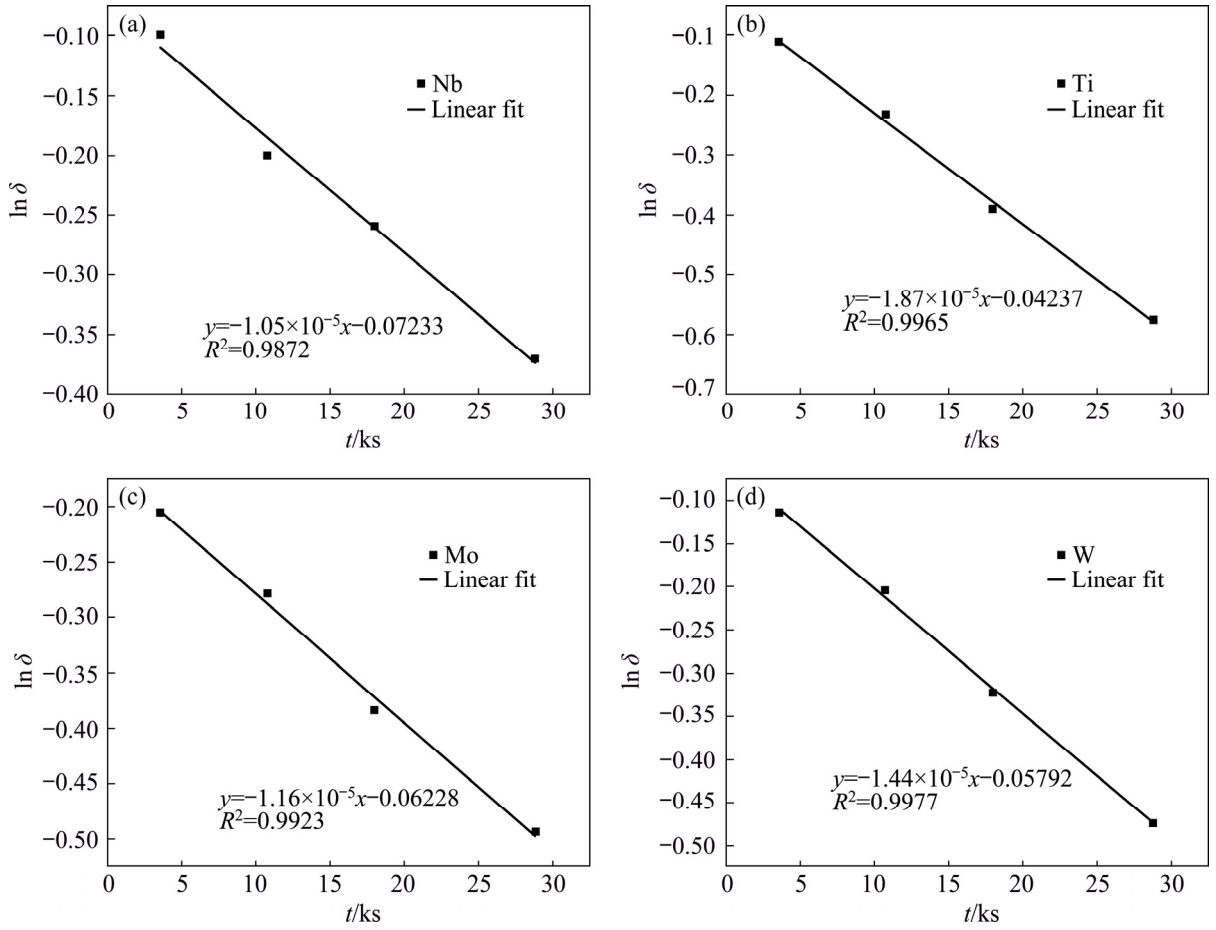

Fig. 13 Linear relationship between ln δ and t for Nb (a), Ti (b), Mo (c) and W (d) homogenized at 1150 °C

4 Conclusions

(1) DSC experiment and metallographic method were applied to determining the incipient melting temperature. And it can be concluded that the IMT of *d*350 mm GH4151 ingot is situated at 1150−1160 °C.

(2) Based on the JMAK analysis at different temperatures, the kinetic equation of Laves phase dissolution can be obtained at the temperatures of 1050, 1100, 1140 and 1150 °C, respectively, and the equations are respectively as follows: X=1−exp(−0.1118$t^{0.73389}$); X=1−exp(−0.2979$t^{0.66695}$); X=1−exp(−0.0.5585$t^{0.56268}$); X=1−exp(−0.7019$t^{0.49318}$).

(3) Based on experiments, the model was verified to be credible to predict the fraction of the dissolution of Laves phase for GH4151 alloy.

(4) The diffusion coefficients of Nb, Ti, Mo, and W were obtained as 2.86×10^{-11}, 5.09×10^{-11}, 3.16×10^{-11}, and 3.92×10^{-11} cm^2/s, respectively, indicating that the diffusion of Nb element is the critical factor for homogenization process of GH4151 alloy.

References

[1] YANG Wan-peng, LI Jia-rong, LIU Shi-zhong, SHI Zhen-xue, ZHAO Jin-qian, WANG Xiao-guang. Orientation dependence of transverse tensile properties of nickel-based third generation single crystal superalloy DD9 from 760 to 1100 °C [J]. Transactions of Nonferrous Metals Society of China, 2019, 29: 558−568.

[2] ZHANG Peng, ZHU Qiang, CHEN Gang, QIN He-yong, WANG Chuan-jie. Grain size based low cycle fatigue life prediction model for nickel-based superalloy [J]. Transactions of Nonferrous Metals Society of China, 2018, 28: 2102−2106.

[3] ZHENG Z, ZHOU J Y, ZHAO W X. Service temperature evaluation of cast K465 superalloy turbine vane based on microstructural evolution [J]. Materials Science Forum, 2019, 944: 411−420.

[4] JIA Chong-lin, ZHANG Feng-lin, WEI Kang, LV Shao-min. Effective solution treatment can result in improved creep performance of superalloys [J]. Journal of Alloys and Compounds, 2019, 770: 166−174.

[5] YIN Bin, XIE Guang, LOU Lang-hong, ZHANG Jian. Abnormal increase of TCP phase during heat treatment in a Ni-based single crystal superalloy [J]. Scripta Materialia, 2019, 173: 1−4.

[6] DUBIEL B, INDYKA P, KALEMBA-REC I, KRUK A. The influence of high temperature annealing and creep on the microstructure and chemical element distribution in the γ, γ' and TCP phases in single crystal Ni-base superalloy [J]. Journal of Alloys and Compounds, 2018, 73: 1693−1703.

[7] RADHAKRISHNA C, PRASADRAO K. The formation and control of Laves phase in superalloy 718 welds [J]. Journal of Materials Science, 1997, 32: 1977−1984.

[8] ZHANG Zhong-kui, YUE Zhu-feng. TCP phases growth and crack initiation and propagation in nickel-based single crystal superalloys containing Re [J]. Journal of Alloys and Compounds, 2018, 746: 84−92.

[9] SAMES W, UNOCIC K, DEHOFF R, LOLLA T, BABU S. Thermal effects on microstructural heterogeneity of Inconel 718 materials fabricated by electron beam melting [J]. Journal of Materials Research, 2014, 29: 1920−1930.

[10] POPP R, HAAS S, SCHERM F, REDERMEIER A. Determination of solubility limits of refractory elements in TCP phases of the Ni−Mo−Cr ternary system using diffusion multiples [J]. Journal of Alloys and Compounds, 2019, 788: 67−74.

[11] WU L M, WANG W H, HSU Y F, TRONG S. Effects of homogenization treatment on recrystallization behavior and dispersoid distribution in an Al−Zn−Mg−Sc−Zr alloy [J]. Journal of Alloys and Compounds, 2008, 456: 163−169.

[12] PAUL D J, CHRISTOPHER J C. Homogenizing a nickel-based superalloy: Thermodynamic and kinetic simulation and experimental results [J]. Metallurgical and Materials Transactions B, 2009, 40: 182−186.

[13] PENG Q Z, ZHOU H T, ZHONG F H, DING H B. Effects of homogenization treatment on the microstructure and mechanical properties of Mg−8Li−3Al−Y alloy [J]. Materials & Design, 2015, 66: 566−574.

[14] CHLEBUS E, GRUBER K, KUźNICKA B, KURZAC J, KURZYNOWSKI T. Effect of heat treatment on the microstructure and mechanical properties of Inconel 718 processed by selective laser melting [J]. Materials Science and Engineering A, 2015, 639: 647−655.

[15] GASKO K L, JANOWSKI G M, PLETKA B J. The influence of γ-γ' eutectic on the mechanical properties of conventionally cast MAR-M247 [J]. Materials Science and Engineering A, 1988, 104: 1−8.

[16] HEGDEA S R, KEARSEYB R M, BEDDOESA J C. Designing homogenization–solution heat treatments for single crystal superalloys [J]. Materials Science and Engineering A, 2010, 527: 5528−5538.

[17] SAMUEL A M, DOTY H W, VALTIERRA S, SAMUEL F H. Defects related to incipient melting in Al−Si−Cu−Mg alloys [J]. Materials & Design, 2013, 52: 947−956.

[18] LASA L, RODRIGUEZ-IBABE J M. Characterization of the dissolution of the Al_2Cu phase in two Al−Si−Cu−Mg casting alloys using calorimetry [J]. Materials Characterization, 2002, 48: 371−378.

[19] MIAO Zhu-jun, SHAN Ai-dang, WU Yuan-biao, LU Jun, XU Wen-liang, SONG Hong-wei. Quantitative analysis of homogenization treatment of INCONEL718 superalloy [J]. Transactions of Nonferrous Metals Society of China, 2011, 21: 1009−1017.

[20] LIFSHITZ I, SLYOZOV V V. The kinetic of precipitation from supersaturated solid solution [J]. Journal of Physics and Chemistry of Solids, 1961, 19: 35−50.

[21] SPRENGEL W, DENKINGER M, MEHRER H. Multiphase diffusion in the Co−Nb and Ni−Nb systems: Part I. Solid-solid phase equilibria and growth of intermetallic phases [J]. Intermetallics, 1994, 2: 127−135.
[22] MIRZADEH H, NAJAFIZADEH A. Aging kinetics of 17-4 PH stainless steel [J]. Materials Chemistry and Physics, 2009, 116: 119−124.
[23] NAJAFIZADEH M, MIRZADEH H. Microstructural Modeling the kinetics of deformation-induced martensitic transformation in AISI 316 metastable austenitic stainless steel [J]. Vacuum, 2018, 157: 243−248.
[24] MIRZADEH H, CABRERA J M, NAJAFIZADEH A, CALVILLO P R. EBSD study of a hot deformed austenitic stainless steel [J]. Materials Science and Engineering A, 2012, 538: 236−245.
[25] SEMIATIN S L, KRAMB R C, TURNER R E. Analysis of the homogenization of a nickel-base superalloy [J]. Scripta Materialia, 2004, 51: 491−495.

一种新型高温合金的初熔相及溶解动力学

李鑫旭[1,2]，贾崇林[2]，张 勇[2]，吕少敏[2]，姜周华[1]

1. 东北大学 冶金学院，沈阳 110819；
2. 中国航发 北京航空材料研究院，北京 100095

摘 要：基于 XRD、SEM 和 EDS 分析，确定 GH4151 合金的组成相。采用差示扫描量热法(DSC)和金相法测定合金的初始熔化温度。结果表明，合金的初熔温度在 1150~1160 ℃之间。随后， 研究 Laves 相的溶解过程，得到不同温度条件下的溶解动力学方程。基于实验，预测 GH4151 合金中 Laves 相溶解分数模型的可靠性得到验证。扩散系数的研究结果表明 Nb 元素的扩散是 GH4151 合金均匀化的关键因素。

关键词：GH4151 铸锭；均匀化；初熔；Laves 相；动力学

(Edited by Xiang-qun LI)